Received: 27 January 2021 | Revised: 10 July 2021 | Accepted: 14 July 2021

DOI: 10.1002/ijc.33756

CANCER GENETICS AND EPIGENETICS

IJC International Journal of Cancer

Definitive evidence for Club cells as progenitors for mutant *Kras/Trp53*-deficient lung cancer

Sebastian Rosigkeit[1] | Marie Kruchem[1] | Dorothe Thies[1] | Andreas Kreft[3] | Emma Eichler[1] | Sebastian Boegel[4] | Sandrine Jansky[1] | Dominik Siegl[1] | Leonard Kaps[1] | Geethanjali Pickert[1] | Patricia Haehnel[5] | Thomas Kindler[5] | Udo F. Hartwig[2,5] | Carmen Guerra[6] | Mariano Barbacid[6] | Detlef Schuppan[1,2,7] | Ernesto Bockamp[1,2]

[1]Institute of Translational Immunology (TIM), University Medical Center, Johannes Gutenberg-University, Mainz, Germany

[2]Research Center for Immunotherapy, University Medical Center, Johannes Gutenberg-University, Mainz, Germany

[3]Institute of Pathology, University Medical Center, Johannes Gutenberg-University, Mainz, Germany

[4]Department of Internal Medicine, University Center of Autoimmunity, University Medical Center, Johannes Gutenberg-University, Mainz, Germany

[5]III. Department of Medicine Hematology, Internal Oncology and Pneumology, University Medical Center, Johannes Gutenberg-University, Mainz, Germany

[6]Experimental Oncology, Molecular Oncology Program, Centro Nacional de Investigaciones Oncológicas (CNIO), Madrid, Spain

[7]Division of Gastroenterology, Beth Israel Deaconess Medical Center, Harvard Medical School, Boston, Massachusetts, USA

Correspondence
Ernesto Bockamp, Institute of Translational Immunology (TIM), University Medical Center, Johannes Gutenberg-University, Mainz, Germany.
Email: bockamp@uni-mainz.de

Funding information
Deutsche Forschungsgemeinschaft; ERAPerMed, Grant/Award Number: ERAPERMED2020-342; Stiftung Rheinland-Pfalz für Innovation, Grant/Award Number: 131838.15

Abstract

Accumulating evidence suggests that both the nature of oncogenic lesions and the cell-of-origin can strongly influence cancer histopathology, tumor aggressiveness and response to therapy. Although oncogenic *Kras* expression and loss of *Trp53* tumor suppressor gene function have been demonstrated to initiate murine lung adenocarcinomas (LUADs) in alveolar type II (AT2) cells, clear evidence that Club cells, representing the second major subset of lung epithelial cells, can also act as cells-of-origin for LUAD is lacking. Equally, the exact anatomic location of Club cells that are susceptible to *Kras* transformation and the resulting tumor histotype remains to be established. Here, we provide definitive evidence for Club cells as progenitors for LUAD. Using in vivo lineage tracing, we find that a subset of $Kras^{12V}$-expressing and *Trp53*-deficient Club cells act as precursors for LUAD and we define the stepwise trajectory of Club cell-initiated tumors leading to lineage marker conversion and aggressive LUAD. Our results establish Club cells as cells-of-origin for LUAD and demonstrate that Club cell-initiated tumors have the potential to develop aggressive LUAD.

Abbreviations: AAHs, atypical adenomatous hyperplasias; ADs, adenomas; AHs, adenomatous hyperplasias; AT2, alveolar type II; BADJs, bronchioalveolar duct junctions; BASCs, bronchioalveolar stem cells; BSA, bovine serum albumin; CAFs, cancer-associated fibroblasts; Cre, Cre-recombinase; EMT, epithelial-to-mesenchymal transition; GEMMs, genetically engineered mouse models; H&E, hematoxylin and eosin; Hmga2, high-mobility group AT-hook 2; *KRAS*, Kirsten rat sarcoma viral oncogene homolog; LacZ, β-galactosidase; LUAD, lung adenocarcinoma; LUSCC, lung squamous cell carcinoma; N/C, nuclear/cytoplasmic; Nkx2-1, NK2 homeobox 1; NSCLC, nonsmall-cell lung cancer; PAS, periodic acid-Schiff; PCR, polymerase chain reaction; SNP, single-nucleotide polymorphism; α-Sma, alpha-smooth muscle actin; Sox2 SRY, (sex-determining region Y)-box 2; SP-C, protein C-expressing; Stk11, serine/threonine kinase 11; TAM, tamoxifen; TBS, Tris-buffered saline; Trp53, tumor suppressor gene 53; X-Gal, 5-bromo-4-chloro-3-indolyl-β-D-galactopyranoside.

KEYWORDS

cell-of-origin, Club cells, genetically engineered mouse model, lung cancer, NSCLC

What's new?

A tumor's cellular origin can influence its histopathology, metastasis, and response to therapy. In this study, the authors provide definitive evidence for Club cells as cells-of-origin for mutant *Kras/Trp53*-deficient lung cancer. In addition, the data identify the specific subgroup of cancer-initiating Club cells that is susceptive to transformation, define their lineage-marker infidelity during tumor progression, and uncover their potential for promoting aggressive lung adenocarcinomas. These results will aid in the understanding of how lung cancer arises and progresses to become a life-threatening condition.

1 | INTRODUCTION

Lung cancer is the most deadly cancer worldwide and mortality rates are rising.[1] Non-small cell lung carcinoma (NSCLC) accounts for ~85% of all lung cancers, with lung adenocarcinoma (LUAD; 40%) and lung squamous cell carcinoma (LUSCC; 30%) comprising its predominant subtypes.[2] Somatic Kirsten rat sarcoma viral oncogene homolog (*KRAS*) mutation represents the most frequent gain-of-function alteration in NSCLC and 40% of *KRAS* mutated NSCLC cases display a second, non-random mutation in the *TP53* tumor suppressor gene (*TRP53*).[3-13] Genetically engineered mouse models (GEMMs) recapitulating these two highly prevalent mutations reproducibly develop lung cancer that resembles human LUAD development.[14-21] Interestingly, generalized expression of oncogenic Kras in the lungs of adult mice initiated tumor formation only in a subset of cells and tissue types.[14,16,18,20] This clearly demonstrated that not all lung cells are amenable to mutant *Kras* transformation and showed that susceptibility to neoplastic transformation depends on anatomical location. To identify the initial source of these tumors, GEMMs with tissue-specific oncogenic *Kras* activation in the absence (K model) of or in conjunction with *Trp53* loss-of-function (KP model) have been used (reviewed in Reference 22). These experiments suggested multiple cell types such as surfactant-associated protein C-expressing (Sftpc thereafter called SP-C) alveolar type II (AT2) cells,[18,20,23-26] secretoglobin-expressing (Scgb1a1 thereafter called CC10) Club cells[20,27] and rare SP-C/CC10 dual positive putative bronchioalveolar stem cells (BASCs)[17] as cells-of-origin for LUAD. While these experiments provided clear evidence for SP-C positive AT2 cells as genuine lung tumor-initiating cells, methodological limitations such as the requirement for initial inflammatory stress caused by infection with adenoviral-Cre-recombinase (Cre) particles[18,20,28] or promiscuous transgene activation in different lung cell types,[24] provided only circumstantial evidence that Club cells indeed act as progenitor cells for K- or KP-promoted LUAD. In addition, Xu and collaborators reported that CC10 single positive Club cells were resistant to $Kras^{12D}$-activated tumor formation due to the lack of concurrent Notch activation.[29] Thus, definitive evidence that *Kras*-transformed Club cells can act as cells-of-origin for LUAD is currently lacking.

Compelling evidence suggests that both the type of oncogenic lesions and the cell-of-origin can strongly influence tumor histotype, local and metastatic dissemination, malignancy and response to therapy.[22,30,31] For example, $Kras^{12D}$-activation together with loss of the serine/threonine kinase 11 (*Stk11* also known as *Lkb1*) tumor suppressor gene function in Club cells induced a mixture of heterogeneous tumor histotypes including lung adenosquamous carcinoma (LUASC), LUSCC and LUAD.[32,33] Similarly, after showing that the initial lung lineage identifiers might be lost during tumor progression, recent studies analyzing single-cell transcript and epigenomic states indicated that KP-transformed AT2 cells progressively adopt alternate lineage identities that resulted in intertumor and intratumor clonal diversity and heterogeneous tumor cell states.[34,35] Although pathologists have stratified human lung cancers on the assumption that neoplastic cells retain features of their cell-of-origin,[2,36] it remains unknown if and which subset of Club cells are susceptible to KP transformation and the ontogeny of putative *Kras*-transformed Club cells has not been sufficiently characterized.

Here, we provide direct experimental proof that mutant $Kras^{12V}$-expressing and *Trp53*-deficient murine Club cells act as progenitors for LUAD. Our study also defines the anatomical location of cancer-initiating Club cells and demonstrates that KP-transformed Club cells lose CC10 lineage marker expression and gradually start to express the AT2 alveolar lineage marker SP-C.

2 | MATERIALS AND METHODS

2.1 | Mice

All animal experiments were in accordance with the local implementation of EU directive 2010/63/EU and were approved by the ethics committee on animal care of Rhineland Palatinate/Germany (Landesuntersuchungsamt Koblenz). The CC10-CreERT2 $Kras^{LSLG12Vgeo/WT}$ $Trp53^{fl/fl}$ (CKP) lung cancer model was homozygous for the CC10-CreERT2(B6N.129S6(Cg)Scgb1a 1tm1(Cre/ERT)Blh/J) knock-in allele,[37] homozygous for the $Trp53^{fl/fl}$ (*Trp*53tm1Brn) knock-in allele[38] and heterozygous for the $Kras^{LSLG12Vgeo}$ knock-in allele.[14] Before the described in vivo lineage tracing experiments, CKP mice were backcrossed to a C57BL/6 background using speed congenic single-nucleotide polymorphism (SNP)-guided crossing (LGC Genomics, Hoddesdon, UK).

2.2 | Genotyping

For genotyping the CC10-CreERT2 allele, we used oligonucleotides 5′-ACTCACTATTGGGGGTGTGG-3′, 5′-AGGCTCCTGGCTGGAATAG-T-3′ and 5′-CCAAAAGACGGCAATATGGT-3′ yielding a 245 bp PCR (polymerase chain reaction) fragment for the CreERT2 knock-in and a 550 bp fragment for the wild-type locus. The *Trp53* allele was genotyped with oligonucleotides 5′-AAGGGGTATGAGGGACAAGG-3′ and 5′-GAAGACAGAAAAGGGGAGGG-3′ yielding a 584 bp fragment for the floxed *Trp53* knock-in and a 431 bp fragment for the wild-type locus. The *Kras*^{LSLG12Vgeo} allele was identified by a three-primer PCR reaction with oligonucleotides 5′-CGTCCAGCGTGTCCTAGACTTTA-3′, 5′-TGACCGCTTCCTCGTGCTT-3′ and 5′-ACTATTTCATACTGGGTCTG-CCTT-3′ yielding a 390 bp knock-in and a 240 bp wild-type fragment.

2.3 | Preparation of tamoxifen working solution and tumor induction

Using a light-tight 50 mL Falcon tube, the tamoxifen (TAM) working solution was prepared by dissolving 1 g TAM (T-5648, Merck Sigma-Aldrich) in 10 mL ethanol at 37°C. Subsequently, 90 mL of autoclaved sunflower oil were added, the mixture placed in a rotating wheel for 15 hours at room temperature and aliquots were stored at −20°C. To induce tumor development, 8-12 weeks old CKP mice received in all cases one injection of 100 μL TAM working solution which corresponds to a total amount of 1 mg TAM per CKP mouse.

2.4 | X-Gal staining and tissue clearing of lungs

X-Gal staining and tissue clearing of whole lungs were performed as described.[39] Briefly, lungs were dissected and fixed in ice-cold acetone, washed twice with PBS and equilibrated at 4°C for 6 hours in equilibration buffer (5 mM potassium ferrocyanide, 5 mM potassium ferricyanide and 2 mM magnesium chloride in PBS pH 7.4). For developing β-galactosidase (*lacZ*) activity, lungs were incubated for 15 hours at 37°C in X-Gal staining buffer (equilibration buffer containing 1 mg/mL X-Gal [5-bromo-4-chloro-3-indolyl-β-D-galactopyranoside dissolved in dimethylformamide]), transferred into post-fixation buffer (4% formaldehyde/1% glutaraldehyde in PBS pH 7.3) and dehydrated in methanol (25%, 50%, 75% and 100%). To render lung tissues transparent, lungs were transferred to a 2:1 mixture of benzyl benzoate/benzyl alcohol at room temperature. After clearing, whole mount images were generated using a Stemi 2000-C binocular (Carl Zeiss, Germany) equipped with a SPOT digital microscope camera (Diagnostic Instruments, Sterling Heights, MI, USA) and imported into Photoshop 7.0 (Adobe Systems, Mountain View, CA). For each analyzed time point, five independent mouse lungs were analyzed ($n = 5$).

2.5 | Preparation and staining of lung tissue sections

For producing paraffin-embedded sections, lungs were dissected, washed twice in PBS and fixed in ice-cold Histofix (Roth, Germany). Subsequently, sections were dehydrated, using a Leica TP1020 automatic benchtop tissue processor (40%-100% ethanol followed by xylene and liquid paraffin). For tissue embedding, a Leica EG1150C cold plate and the Leica EG1150H heated paraffin-dispensing module were used. Sections of 5 μm thickness were produced with a Leica RM2255 rotary microtome, deparaffinized (65°C for 1 hour), and stained with hematoxylin and eosin (H&E).

To visualize *lacZ* reporter gene activity on sections, lungs were inflated with fixation buffer (2% [w/v] 0.25% glutaraldehyde in PBS pH 7.4), incubated in fixation buffer for 2 hours at room temperature, transferred into equilibration buffer (5 mM potassium ferrocyanide, 5 mM potassium ferricyanide and 2 mM magnesium chloride in PBS pH 7.4), and placed for a minimum of 3 hours on a rocking platform (4°C; 100-200 rpm). Next, lungs were transferred into X-gal staining solution (equilibration buffer containing 1 mg/mL X-Gal) and placed on a rocking platform (37°C; 100 rpm) for 12 hours. Finally, lungs were washed once in PBS for 5 minutes and fixed overnight at 4°C in PBS containing 4% paraformaldehyde and embedded in paraffin.

2.6 | Immunohistochemistry

Lungs were harvested, stained, fixed and paraffin-embedded as described. To remove all traces of paraffin, sections were subjected to two consecutive xylol incubation steps (2× 10 minutes). Deparaffinized sections were rehydrated (2× 100% isopropanol for 10 minutes, 2× 95% isopropanol for 10 minutes, 2× 75% isopropanol for 10 minutes and 2× distilled H_2O for 5 minutes), followed by antigen retrieval (10 mM sodium citrate buffer pH 6.0/steam cooker for 30 minutes) and washed in distilled H_2O for 5 minutes. To block endogenous peroxidase activity, tissue sections were incubated with 3% hydrogen peroxide in distilled H_2O for 15 minutes and washed in distilled H_2O (2× 5 minutes). To permeabilize cells, sections were incubated twice for 10 minutes in permeabilization buffer (1% bovine serum albumin (BSA) in tris-buffered saline pH 7.6 (TBS) containing 0.4% Triton X-100). Blocking was performed with 2.5% normal horse serum (Vector Laboratories, Burlingame, CA) for at least 1 hour.

In all cases, primary antibodies (Table 1) were diluted in TBS-T (1% bovine serum albumin in TBS containing 0.1% Triton X-100), added to the sections and incubated in a dark humid chamber at 4°C overnight.

After washing twice in TBS-T for 10 minutes, secondary antibodies were applied. In case primary rabbit antibodies were used, sections were incubated with an HRP-labeled secondary goat anti-rabbit IgG antibody for 1-2 hours. Sections were washed for 10 minutes in TBS-T, submitted to DAB staining (IMPACT DAB Kit, Vector Laboratories, SIC_4105) and washed in tap water. In case primary rat

TABLE 1 Detailed list of antibodies used for immunochemistry

Antigen	Antibody	Source	Article no.	Dilution
SP-C	Recombinant anti-SP-C antibody	Abcam	ab211326	1:1000
CC10 (Scgb1a1)	Anti-CC10 antibody	Abcam	ab40873	1:300
SOX2	Anti-Sox2 antibody	Abcam	ab97959	1:200
NKX2-1	Recombinant anti-*Nkx*2-1 antibody	Abcam	ab76013	1:1000
Ki67	Anti-Ki67 antibody	Bethyl	IHC-00375	1:500
Vimentin	Anti-vimentin antibody	Abcam	ab92547	1:1000
CD45	Anti-mouse CD45	Biolegend	103 101	1:200
Hmga2	Anti-Hmga2 antibody	Abcam	ab97276	1:100
α-Sma	Anti-α-Sma	Abcam	ab124964	1:1000
IgG rabbit	Goat anti-rabbit IgG heavy and light chain (HRP)	Abcam	ab205718	1:10000
IgG rat	Goat anti-rat IgG heavy and light chain (biotinylated)	Vector laboratories	BA-9401	1:1000

antibodies were used, sections were incubated with a biotinylated anti-rat IgG for 1-2 hours. Sections were washed for 10 minutes in TBS-T, and submitted first to an ABC Kit (VECTASTAIN Elite, Peroxidase, PK-6100) signal amplification step, followed by DAB staining (IMPACT DAB Kit, Vector Laboratories, SIC_4105) and washed in tap water. Slides were developed by adding 200 μL DAB solution, counterstained with hematoxylin (Roth, Germany) and dipped into tap water for stopping hematoxylin staining. Finally, sections were dehydrated using incubation steps (each 10 min, 95% ethanol, 100% ethanol and 2× xylene), mounted with Roti Histokit II, sealed with coverslips and documented using an AxioScope.A1 microscope (Zeiss, Germany).

2.7 | Periodic acid Schiff staining

For periodic acid Schiff (PAS) staining 5 μm deparaffinized lung sections were placed in 1% periodic acid (Roth, Germany, HP00.1) for 10 minutes, washed in tap water for 5 minutes, rinsed in distilled water and treated with Schiff's reagent (Roth, Germany, X900.2) for 20 minutes at room temperature. Next, sections were washed in tap water for 5 minutes, rinsed in distilled water and counterstained with Mayer's hemalum solution for 7 seconds (Merck, Germany, 1.09249.2500). Hemalum staining was stopped by washing with tap water and rinsing with distilled water as above. Slides were dehydrated and mounted with a coverslip.

2.8 | Quantitative analysis of lung tissue sections

Quantitative analysis of H&E-stained and anti-CC10, anti-SP-C, anti-Nkx2-1 and anti-Sox2 antibody-stained sections was in all cases performed using a minimum of three individual tissue sections with each consecutive section having a distance of ≥100 μm to the previous section for each individual mouse (n = 5 mice). For each time point (control, 12 days, 2, 4 and 5 months after TAM) five individual CKP lungs were analyzed. For determining the number of AHs, AAHs (diameter < 100 μm) and ADs (diameter > 100 μm), paraffin-embedded H&E-stained whole mouse lungs were used. For antibody-stained sections, whole lungs were first X-Gal-stained, embedded in paraffin, sectioned, deparaffinized, incubated with primary and secondary antibody as described above, counterstained with hematoxylin, and recorded using an AxioScope.A1 microscope (Zeiss, Germany).

For documenting H&E-stained whole lung lobe sections, paraffin-embedded slides (2, 4 and 5 months after tumor induction) were scanned using a NanoZoomer 2.0-HT slide scanner (Hamamatsu Photonics, Hamamatsu City, Japan). Sections were analyzed with the NDP view 3.1.66 software (Hamamatsu Photonics, Japan).

For defining N/C ratios, we used the Zeiss ZEN analysis software (Zeiss, Germany).

2.9 | TCGA analysis

TCGA data was retrieved using the R package TCGAbiolinks. Code (6f5cde97-d259-414f-8122-6d0d66f49b74). To compare the patient dataset to the here used CKP mouse model, only *KRAS* and *TP53* co-mutated (all mutations and deletions included) patients have been analyzed. Gene expression levels from CC10 (ENSG00000149021) and SP-C (ENSG00000168484) were derived and depicted on log10 scale.

3 | RESULTS

3.1 | Progressive lung tumorigenesis is reproducibly induced in CKP mice

To initiate lung tumor development, we used CC10-CreERT2 $Kras^{LSLG12Vgeo/WT}$ $Trp53^{fl/fl}$ (CKP) GEMMs. In CKP mice, tamoxifen (TAM) injection induces conditional expression of oncogenic $Kras^{12V}$ that is co-expressed with the *β-Geo lacZ* reporter gene, and concurrently inactivates *Trp53* tumor suppressor function (Figure 1A).

As depicted in the transparent whole lung images of Figure 1B, a single dose of 1 mg TAM produced a characteristic blue pattern of recombined *lacZ*-expressing cells that become visible after incubation with 5-bromo-4-chloro-3-indolyl-β-D-galactopyranoside (X-Gal). Twelve days after TAM injection, X-Gal staining highlighted the pseudostratified columnar lung epithelium of the bronchi and the preterminal and distal bronchioles. This characteristic pattern was almost identical at 2 months and at 4 months after TAM injection, multiple blue-stained hyperplastic areas, several small and some larger tumors had developed. As shown in the left image of Figure 1B, lung lobes from CKP mice never receiving TAM completely lacked X-Gal-stained *Kras*^{12V}-expressing cells. This initial analysis indicated that CKP mice receiving a single TAM injection reproducibly develop a distinctive pattern of progressive lung tumorigenesis.

3.2 | Low-dose tamoxifen directs conditional gene activation to Club cells in CKP mice

Lineage tracing experiments with the CC10-CreERT2 mouse strain could not conclusively define *Kras*-initiated lung cancer progenitors because in these experiments TAM application caused conditional gene activation in Club cells, AT2 cells and presumptive BASCs.[24] Assuming a possible dose-response effect, we wondered if reducing the amount of TAM could restrict Cre-recombinase activity to Club cells in CKP mice. To test this hypothesis and to determine the identity of lung cells that had undergone Cre-mediated recombination, we X-Gal stained proximal and distal lung sections of CKP mice that received a single injection of 1 mg TAM. As shown in the microscopic images of Figure 2A-C, at day 12 after TAM induction epithelial cells lining the proximal large airways, as well as cells in the distal bronchioles and bronchioalveolar duct junctions (BADJs) had undergone Cre-recombination reaching a recombination efficiency of 95%. In contrast, alveolar spaces did not contain any recombined *lacZ*-expressing cells (Figure 2D). To further confirm the targeting selectivity, we applied lineage-specific antibodies. Staining for CC10 protein expression overlapped with recombined Club cells in the large airways, the bronchioles and the BADJs (Figure 2E-G) but did not stain AT2 cells in the alveoli (Figure 2H). In contrast, recombined *lacZ*-expressing cells did not express SP-C protein (Figure 2I-K). As expected, *lacZ*-negative AT2 cells expressed the SP-C marker (Figure 2L). Although short TAM serum half-life times of about 12 hours have been reported for rats and mice[40] and 1 mg TAM injection reproducibly directed Cre-recombination to Club cells but not to BASCs and AT2 cells at day 12, we wanted to confirm the absence of recombination in AT2 cells and BASCs at a later time point. As shown in Figure S1, injection of 1 mg TAM equally failed to induce recombination in SP-C^{+} AT2 cells and CC10/SP-C dual positive BASCs at day 20. The observed staining of recombined cells with CC10 antibodies thus demonstrated that the low-dose TAM regime applied directs oncogenic *Kras*^{12V} expression to CC10 single positive Club cells but not to AT2 cells and CC10/SP-C dual positive BASCs in

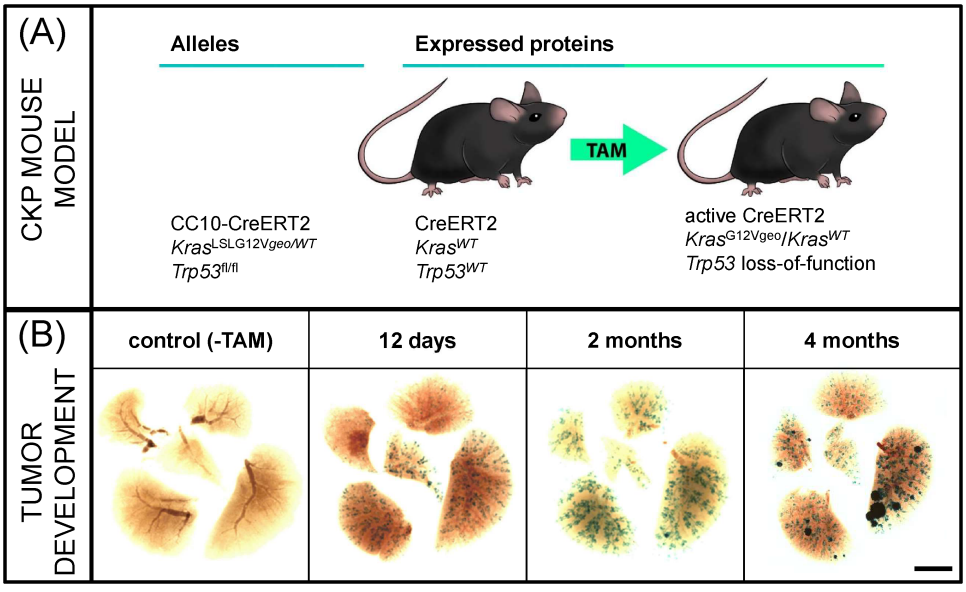

FIGURE 1 Conditional expression of oncogenic *Kras*^{12V} and inactivation of *Trp53* tumor suppressor function promotes progressive lung tumorigenesis in CKP mice. A, Schematic representation depicting tamoxifen (TAM)-induced conditional transgene activation in the CKP mouse model. In CKP mice, the CreERT2 coding sequence is under the transcriptional control of the endogenous CC10 promoter. After TAM injection, CKP mice start to express oncogenic *Kras*^{12V} together with the *β-Geo lacZ* reporter gene and concomitantly lose *Trp53* tumor suppressor function. B, Representative images of CKP lungs demonstrating progressive lung tumorigenesis after TAM injection. The images show all five lung lobes as transparent X-Gal-stained whole mounts obtained from CKP mice before (control) and at 12 days, 2 months and 4 months after a single intraperitoneal injection of 1 mg TAM. Lung lobes shown are the right-lung cranial lobe, the right-lung middle lobe, the right-lung post caval lobe, the left-lung lobe and the right-lung caudal lobe. A similar tumor progression pattern was observed using additional TAM-induced CKP lungs (n = 5 mice). Bar represents 2 mm [Color figure can be viewed at wileyonlinelibrary.com]

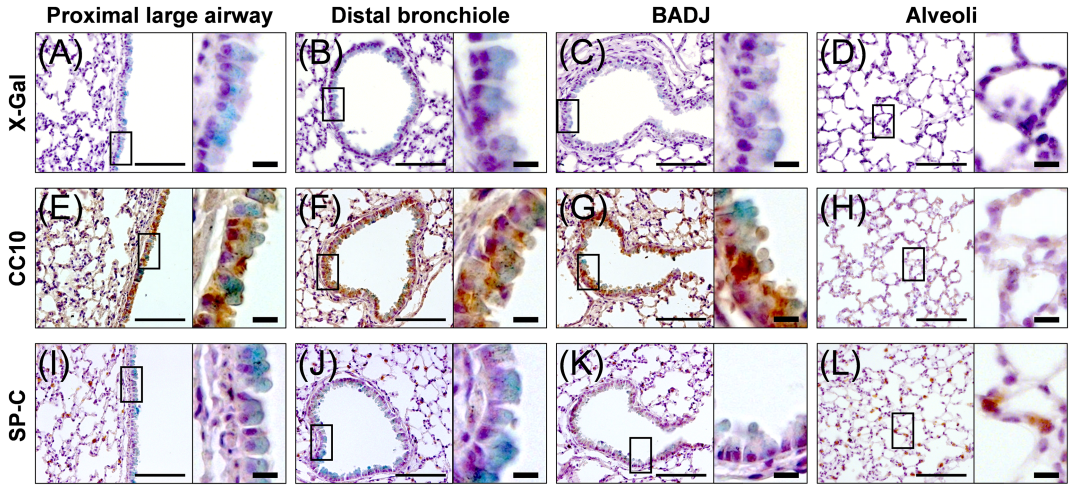

FIGURE 2 Low-dose TAM induction directs *Kras*^{12V} expression to CC10 single positive Club cells. A-D, Photomicrographs of representative X-Gal-stained lung sections from CKP mice at day 12 after TAM induction. Rearranged *Kras*^{12V}-*β-Geo lacZ*-expressing cells are X-Gal-stained in blue at the proximal large airways (A), the distal bronchioles (B) and the BADJs (C) but not in the alveoli (D). E-H, Immunodetection of CC10-expressing cells on X-Gal-stained CKP lung sections at day 12 after TAM induction. Representative photomicrographs demonstrating the expression of the Club cell-specific CC10 protein in rearranged X-Gal^{+} cells of the proximal airways (E), the distal bronchioles (F), the BADJs (G) and the absence of CC10^{+} cells in the alveoli (H). I-L, Immunodetection of SP-C-expressing cells on X-Gal-stained CKP lung sections at day 12 after TAM induction. Representative photomicrographs demonstrating the lack of SP-C protein expression in rearranged X-Gal^{+} cells of the proximal airways (I), the distal bronchioles (J) the BADJs (K) and the presence of SP-C^{+} AT2 cells in the alveoli (L). Thin bars represent 100 μm and thick bars represent 10 μm. For each analysis, similar results were obtained using additional TAM-induced lungs (n = 5 mice) [Color figure can be viewed at wileyonlinelibrary.com]

CKP mice. Because the NK2 homeobox 1 (*Nkx2-1*, also known as *Ttf-1*) transcription factor is a common classifier for human LUAD[41,42] that is expressed in >70% of patients[43,44] and has been described to act as an oncogene in *TRP*53-mutated lung adenocarcinomas,[45] we next documented Nkx2-1 expression in normal lungs and at 12 days after TAM injection. As shown in Figure S2A-D, in normal lungs Nkx2-1 protein was uniformly expressed in epithelial cells of the large airways, the distal bronchioles, the BADJs and in alveolar AT2 cells. Likewise, at 12 days after TAM injection, the vast majority but not all recombined Club cells of the large airways, the distal bronchioles and the BADJs expressed Nkx2-1 in CKP mice (Figure S2E-G). Since the SRY (sex-determining region Y)-box 2 (Sox2) transcription factor is implicated in oncogenic lineage specification, reprogramming and therapeutic resistance,[46-50] we next investigated if oncogenic *Kras* expression/*Trp53*-deletion in Club cells induces Sox2 expression. As expected Sox2 was expressed in basal cells but we did not detect any Sox2 protein in recombined Club cells (Figure S2H-J). We conclude that low-dose TAM induction directs oncogenic *Kras*^{12V} activation to CC10 single positive Club cells in CKP mice and that Nkx2-1 and Sox2 expression is basically not altered in mutant *Kras*-expressing/*Trp53*-deleted Club cells.

3.3 | Club cell-derived preneoplastic areas are restricted to distal bronchioles

Having demonstrated that a low-dose TAM regime directs conditional gene activation to CC10 single positive Club cells, we next wanted to identify the anatomical localization of presumptive cancer-initiating cells. Because proliferation is a necessary condition for the development of preneoplastic lesions, we investigated the location of proliferating cells among *Kras*^{12V}-transformed/*Trp53*-deleted cells. To this end, we stained proximal and distal lung sections from normal and from CKP mice at 12 days after TAM induction with Ki67 antibodies. As shown in Figure S3A, epithelial cells lining the proximal airways did not, or only very rarely, stain for the Ki67 proliferation marker in wild-type mice. In contrast, we found Ki67^{+} cells within the distal bronchioles, in proximity to the BADJs and in the alveoli (Figure S3B-D). Interestingly, microscopic analysis of lung sections from TAM-induced CKP mice produced a very similar distribution pattern with proliferating cells confined to the distal bronchioles, the BADJs and the alveoli (Figure S3E-H). To provide additional evidence for the distal anatomical localization of preneoplastic cells, we examined X-Gal-stained lung sections for the presence of Ki67^{+} areas at 2 months after TAM injection. While proximal airways, BADJs and alveolar spaces did not show signs for proliferative preneoplastic areas (Figure S1I, K and L), clusters of preneoplastic cells frequently localized to the distal bronchioles (Figure S3J). These findings show that expression of oncogenic *Kras*^{12V} together with *Trp53* loss-of-function promotes preneoplastic growth only in a subset of Club cells and that these cells are localized to the distal bronchioles.

3.4 | Proliferating preneoplastic Club cells progressively lose CC10 lineage marker expression

To gain insight into early histopathological alterations, we next analyzed CKP lungs at 2 months after TAM injection. At this time,

transparent X-Gal-stained lungs preserved the initial characteristic pattern of recombined cells observed 12 days after TAM application (Figure 1). However, at 2 months several enlarged X-Gal-stained areas of different sizes appeared in the distal lungs. Hematoxylin and eosin (H&E) staining revealed that these areas consisted of 93% adenomatous hyperplasias (AHs) and atypical adenomatous hyperplasias (AAHs) and 7% larger (ADs, diameter > 100 μm) adenomas (Figure S4A and B). These early lesions showed mild nuclear atypia such as enlarged nuclei, intermediate nuclear/cytoplasmic (N/C) ratios, fine granular chromatin and distinct small nucleoli but lacked invasive growth patterns (Figure S4C and D). In addition, we did not find any infiltration with immune cells in AHs, AAHs and ADs (Figure S5).

Human LUAD tumors are reported to change their initial histotype and have the ability to shift lineage marker expression during disease progression and upon therapy.[51,52] In support of additional evidence for histotype plasticity, KP-transformed murine AT2 lung cancer cells progress through a continued evolution of increased heterogeneity and clonal diversification.[34,35] Therefore, we wondered if KP-transformed Club cells might undergo a similar degree of plasticity. To assess bronchiolar vs alveolar lineage marker identity, we investigated CC10- and SP-C-expression at 2 months after tumor initiation. Interestingly, staining with either CC10 or SP-C antibodies demonstrated the presence of both CC10 and SP-C positive lesions (Figure 3A, B, D and E). Of all AHs, AAHs and ADs, 23% retained CC10 expression (Figure 3C) and 76% had started to express SP-C (Figure 3F). Further indicating the early diversification of transformed Club cells, we found that 24% of all preneoplastic lesions had completely lost initial Nkx2-1 transcription factor expression (Figure S6A-C). However, at this early stage of tumorigenesis, we did not observe lesions with Sox2 protein expression (Figure S6D-F).

These results show that KP-transformed CC10 single positive preneoplastic Club cells have the ability to generate AHs, AAHs and ADs lacking apparent immune cell infiltration. Our findings also demonstrate that the developing lesions do not strictly preserve CC10 expression but start to express SP-C protein, which is a marker for alveolar lineage specification and identity.

3.5 | Disease progression promotes LUAD consisting of heterogeneous cancer cells

Given the immediate shift in lineage-defining markers, we wanted to investigate the intrinsic propensity of KP-transformed Club cells to fuel continued lung carcinogenesis and to progressively generate tumors with lineage marker conversion. To this end, we analyzed lungs at 4 months after TAM injection. At this time point, CKP lungs presented numerous variably sized lesions including several larger tumors (Figure 1B). Indicating continuous tumor progression, 20% of these lesions were adenomas (ADs, diameter > 100 μm) and 80% AHs and AAHs (Figure S7A and B). Some of the bigger lesions also started to display characteristic features of mouse LUAD. For example, we found multiple larger adenocarcinomas (ACs; diameter > 500 μm) with papillary growth patterns (Figure S7C). In comparison to 2 months,

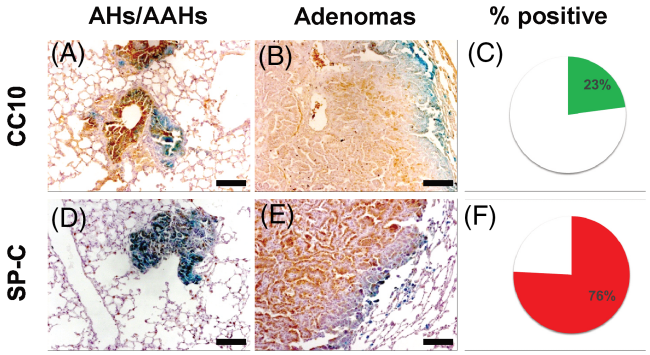

FIGURE 3 Club cell-initiated tumors lose CC10 expression and start to express the AT2 cell marker SP-C. A-B, Photomicrographs showing CC10 expression in AHs/AAHs and adenomas at 2 months after TAM injection. Bars represent 100 μm. C, Percentage of $CC10^+$ AHs/AAHs and adenomas at 2 months after TAM injection. D-E, Photomicrographs showing SP-C expression in AHs/AAHs and adenomas at 2 months after TAM injection. Bars represent 100 μm. F, Percentage of $SP\text{-}C^+$ AHs/AAHs and adenomas at 2 months after TAM injection. Similar results for all readouts were obtained using additional TAM-induced lungs (n = 5, mice) [Color figure can be viewed at wileyonlinelibrary.com]

cancer cells were increasingly pleomorphic displaying striking nuclear hyperchromasia, large round nuclei, reduced N/C ratios and bigger nucleoli, and we occasionally found multinuclear giant cancer cells (Figure S7D). Nonetheless, all lesions lacked obvious immune cell infiltration but extra-tumoral $CD45^+$ immune cell clusters sporadically surrounded larger ADs (Figure S8A and B). Immunohistochemical analysis of AHs, AAHs, ADs and ACs further revealed that the number of lesions containing CC10-expressing cancer cells remained low (20%) while an increasing number of lesions harbored SP-C-expressing cancer cells (73%; Figure 4A-H). In addition, the number of lesions with $Nkx2\text{-}1^+$ cells further decreased (66%) and for the first time, we identified tumors (5%) containing Sox2 protein expressing cells (Figure 4I-P). Immunostaining for CC10 and SP-C of consecutive lung tumor sections further confirmed the intertumoral and intratumoral heterogeneity of CC10 and SP-C lineage marker expression. At this time, we found (a) tumors expressing both CC10 and SP-C, (b) tumors harboring cells preserving CC10 expression that have started to express SP-C in a subset of cells and (c) $SP\text{-}C^+$ tumors lacking CC10 expression (Figure S9). These results demonstrate the existence of a developmental oncogenic program promoting an initially papillary LUAD histotype of intertumoral and intratumoral heterogeneity, characterized by the maintenance of $Nkx2\text{-}1^+$ lesions, the continued decrease of $CC10^+$ lesions, an increase in $SP\text{-}C^+$ lesions and the emergence of some $Sox2^+$ tumors.

3.6 | Club cell-initiated tumors become increasingly malignant

Previous data suggested that activation of mutant *Kras* in Club cells does not promote malignant late-stage tumor formation.[18,24,26]

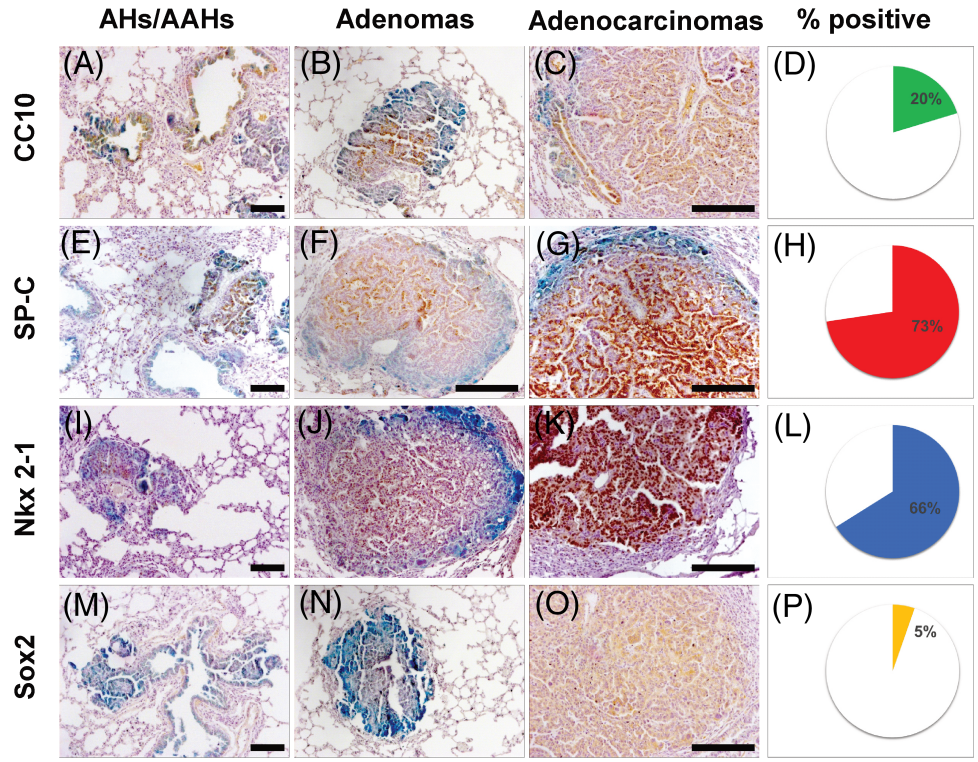

FIGURE 4 Bronchiolar and alveolar lineage marker expression and gain of Sox2 transcription factor expression at 4 months after tumor initiation. A-C, Photomicrographs showing CC10 expression in AHs/AAHs, adenomas and adenocarcinomas at 4 months after TAM injection. Small and large bars represent 100 μm. D, Percentage of $CC10^+$ AHs/AAHs and adenomas at 4 months after TAM injection. E-G, Photomicrographs showing SP-C expression in AHs/AAHs, adenomas and adenocarcinomas at 4 months after TAM injection. Small and large bars represent 100 μm. H, Percentage of $SP\text{-}C^+$ AHs/AAHs, adenomas and adenocarcinomas at 4 months after TAM injection. I-K, Photomicrographs showing Nkx2-1 expression in AHs/AAHs, adenomas and adenocarcinomas at 4 months after TAM injection. Small and large bars represent 100 μm. L, Percentage of $Nkx2\text{-}1^+$ AHs/AAHs, adenomas and adenocarcinomas at 4 months after TAM injection. M-O, Photomicrographs showing Sox2 expression in AHs/AAHs, adenomas and adenocarcinomas at 4 months after TAM injection. Small and large bars represent 100 μm. P, Percentage of $Sox2^+$ AHs/AAHs, adenomas and adenocarcinomas at 4 months after TAM injection. Similar results for all readouts were obtained using additional TAM-induced lungs (n = 5 mice) [Color figure can be viewed at wileyonlinelibrary.com]

To determine if KP-transformed Club cells have the potential to generate malignant LUAD, we analyzed CKP lungs at 5 months after TAM injection, at which point several larger tumors (diameter between 500 and 2500 μm) had developed (Figure 5A). Inspection of diseased lungs showed clear histopathological features of malignancy. As illustrated in Figure 5A, at 5 months after TAM induction, big tumors constituted the most prevalent tissue element in some lung areas. Further indicating a heterogeneous and aggressive LUAD phenotype, tumors displayed regional variation consisting of acinar or papillary growth patterns of differentiated and highly pleomorphic areas (Figure 5B-D). Detailed examination of individual cancer cells exhibited severe and variable nuclear atypia, with large heterochromatic nuclei, coarse granular chromatin and high N/C ratios (Figure 5E,F). At this stage, we also identified sporadic nuclear pseudo-inclusions and multi-nucleated giant cancer cells (Figure S10A,B). Indicative of productive tumor establishment, some bigger ACs had intratumoral blood vessel supplies while other larger ACs were regressive, lacking sufficient blood supply (Figure S10C,D). Although both smaller lesions and bigger ACs contained hardly any infiltrating $CD45^+$ immune cells, some larger tumors were flanked by neighboring immune cell clusters (Figure S11A,B).

Indicating an almost complete lineage marker conversion, immunostaining with CC10 and SP-C antibodies revealed that only a fraction of tumors contained $CC10^+$ cells (6%), while nearly all tumors (98%) now expressed SP-C protein (Figure 6A-F). Moreover, we found Nkx2-1 transcription factor expression in almost all tumors (93%; Figure 6G-I). Further confirming progressive cellular diversification, at 5 months after TAM induction, about half of all tumors (51%) contained transformed cells expressing the Sox2 transcription factor (Figure 6J-L). To show the progressive alterations in CC10, SP-C, Sox2 and Nkx2-1 protein expression, Figure S12 summarizes these data. However, we never detected PAS-stained cancer cells within these heterogeneous tumors indicating the absence of a mucinous LUAD histotype (Figure S13A-C). Finally and indicating the absence of tumor cells starting to undergo epithelial-to-mesenchymal transition (EMT), larger tumors never contained regional foci of vimentin-expressing cells at this time point (Figure S13D,E). Indicative for the presence of cancer-associated fibroblasts (CAFs), we found high levels of alpha-smooth muscle actin (α-Sma) protein in and around larger tumors (Figure S13F,G). Equally, all larger tumors expressed high-mobility group AT-hook 2 (Hmga2) protein (Figure S14A-D), a marker

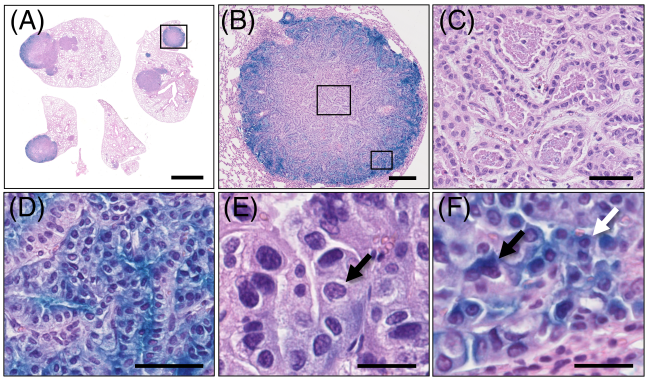

FIGURE 5 Club cell-initiated tumors progress to malignant LUAD. A, Representative H&E-stained lung section from CKP mice at 5 months post tumor initiation. Black frame indicates the position of the mid-sized adenocarcinoma shown in B. Scale bar represents 1 mm. B, Adenocarcinoma with papillary and acinar growth pattern. Upper black frame indicates the enlarged picture detail of (C) and lower black frame the enlarged picture detail of Figure 6D. Scale bar represents 200 μm. C, Tumor area with acinar growth pattern. Scale bar represents 50 μm. D, Tumor area with papillary growth pattern. Scale bar represents 50 μm. E, Photomicrograph showing cancer cells with large nuclei with high N/C ratios of variable size and heterochromatic nucleoli (black arrow). Scale bar represents 25 μm. F, Photomicrograph showing variable nuclear atypia with small (white arrow) and large nuclei (black arrow). Scale bar represents 25 μm. Similar results for all readouts were obtained using additional TAM-induced lungs (n = 5 mice) [Color figure can be viewed at wileyonlinelibrary.com]

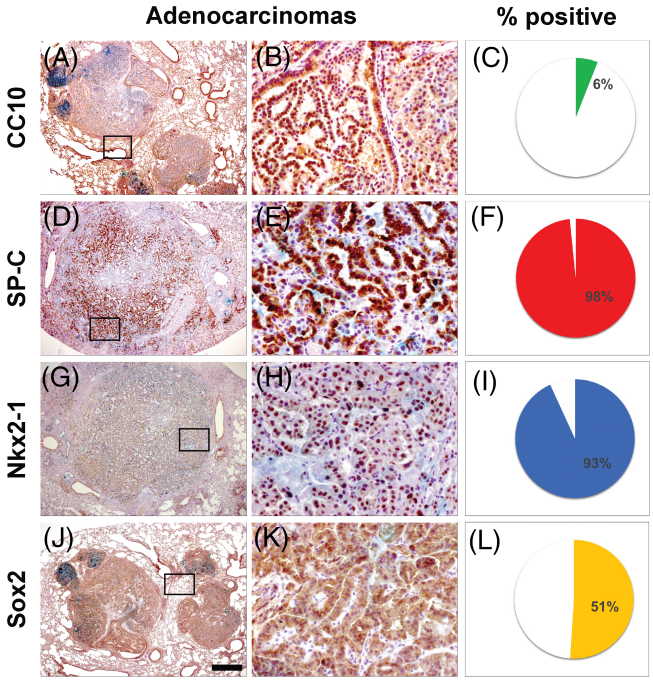

FIGURE 6 Most Club cell-derived adenocarcinomas have lost the CC10 lineage marker, express SP-C and start to contain Sox2 positive cancer cells. A-B, Photomicrographs showing CC10 expression in an adenocarcinoma at 5 months post tumor initiation. Black frame in A indicates the position of the enlarged detail in B. Small bar represents 400 μm and large bar 100 μm. C, Percentage of all $CC10^+$ lesions at 5 months after TAM injection. D-E, Photomicrographs showing SP-C expression in an adenocarcinoma at 5 months post tumor initiation. Black frame in D indicates the position of the enlarged detail in E. Small bar represents 400 μm and large bar 100 μm. F, Percentage of $SP\text{-}C^+$ lesions at 5 months after TAM injection. G-H, Photomicrographs showing Nkx2-1 expression in an adenocarcinoma at 5 months post tumor initiation. Black frame in G indicates the position of the enlarged detail in H. Small bar represents 400 μm and large bar 100 μm. I, Percentage of $Nkx2\text{-}1^+$ lesions at 5 months after TAM injection. J-K, Photomicrographs showing Sox2 expression in an adenocarcinoma at 5 months post tumor initiation. Black frame in J indicates the position of the enlarged detail in K. Small bar represents 400 μm and large bar 100 μm. L, Percentage of $Sox2^+$ lesions at 5 months after TAM injection. Similar results for all readouts were obtained using additional TAM-induced lungs (n = 5 mice) [Color figure can be viewed at wileyonlinelibrary.com]

that has been recently reported to indicate stages of advanced tumor malignancy.[35]

Analysis of late stage sections thus showed the potential of *Kras*^{12V}-expressing and *Trp53*-deleted Club cells to generate malignant tumors in our model. The intertumoral and intratumoral diversity of progressed tumors further demonstrated that initially KP-transformed Club cells undergo a progressive lineage marker conversion toward alveolar AT2-type specification that is accompanied by nearly uniform Nkx2-1 and newly acquired Sox2 transcription factor expression in the majority of advanced tumors.

3.7 | The majority of LUAD patients express CC10 during early stages of tumor development

Human LUAD tumors have been reported to change their initial histotype and have the ability to shift lineage marker expression during disease progression and upon therapy.[51,52] To investigate CC10 and SP-C linage marker expression in human LUAD patients, we analyzed mRNA-Seq data from The Cancer Genome Atlas (TCGA).[53] This analysis revealed that from 548 samples, 34 carried the KP mutation. As shown in Figure S15A, from all Stage I KP lung tumor biopsies, nine had high (9/18; 50%), seven intermediate (7/18; 39%) and two low (4/18; 11%) CC10 mRNA levels. In Stage II samples, the percentage of high CC10 mRNA biopsies decreased (2/8; 25%) and a higher proportion of samples displayed intermediate (4/8; 50%) and low (2/8; 25%) CC10 mRNA levels. Of the five Stage III patients, two had high (2/5; 40%), two intermediate (2/5; 40%) and one low (1/5; 20%) CC10 mRNA levels. We also observed an additional overall reduction of CC10 mRNA in Stage IV biopsies with two patients (2/3; 66%) showing intermediate and one patient (1/3; 33%) low levels. Analysis of SP-C expression in the same cohort (Figure S15B) revealed that the majority of Stage I biopsies contained high (9/18; 50%) or intermediate (7/18, 38%) SP-C mRNA levels with only four patients (4/18, 22%) expressing low amounts of SP-C mRNA. In Stage II biopsies, the percentage of SP-C high (2/8; 25%) and intermediate (2/8; 25%) expressers dropped and a higher patient fraction expressed low (4/8;

50%) SP-C mRNA. Of the five Stage III patients, two had high (2/5; 40%) one intermediate (1/5; 20%) and two low (2/5; 40%) SP-C mRNA levels. Late Stage IV samples either contained high (2/3; 66%) or intermediate (1/3; 33%) SP-C mRNA levels.

To visualize CC10 and SP-C co-expression, Figure S15C shows a weighted mRNA level plot displaying CC10 and SP-C mRNA recordings for each individual patient sample. Interestingly, CC10 (16/18; 89%) and SP-C levels (14/18; 78%) were high to intermediate in the majority of Stage I samples with only two patients expressing low amounts of CC10 and SP-C mRNA (2/18; 11%). Samples from Stage II and Stage III patients were less uniform and contained fewer patients with high CC10 (Stage II 2/8; 25% and Stage III 1/5; 20%) and SP-C (Stage II 2/8; 25% and Stage III 1/5; 20%) mRNA. From the three Stage IV patient biopsies listed in the TCGA, two expressed intermediate (2/3; 66%) and one low (1/2; 33%) amounts of CC10 while SP-C mRNA levels were high in two (2/3; 66%) and intermediate in one (1/3; 33%) patient. Although only based on a small number of samples, the analysis of KP-mutated human LUAD tumors clearly demonstrated the high to intermediate co-expression of CC10 and SP-C lineage markers at early stages of disease. In addition, overall CC10 mRNA was reduced and SP-C expression remained high or intermediate in a small cohort of three Stage IV patients. Thus, the initially high CC10 levels, the heterogeneous co-expression of CC10 and SP-C lineage markers and the late decrease of CC10 is similar in CKP mice and human patients. Because the cell-of-origin and the developmental dynamic of individual TCGA patients are unknown, the suggestive resemblance of CC10 and SP-C lineage marker expression between CKP mice and human patients should be interpreted with appropriate caution.

4 | DISCUSSION

One of the central issues facing cancer research is to understand how cancer arises and progresses to become a life-threatening condition. Given that nonrandom *TRP53* mutations occur in about 40% of KRAS-mutated Caucasian[3-13] and to a lower degree in Chinese[54] LUAD patients, we here investigated the oncogenic role of these co-occurring lesions in murine Club cells. Besides the ability of genetic alterations to promote cancer, emerging evidence from clinical data and experiments in mice suggests a direct link between the cell-of-origin, the resulting pathology, the tumor histotype and the response to therapy in some cancer types including lung cancer.[22,30,31] Our data demonstrate that KP murine Club cells act as progenitors for aggressive LUAD. Using lineage tracing and single-cell recording, we further establish the anatomic localization of LUAD-initiating Club cells to the distal bronchioles. Moreover, considering the existence of a progressively unfolding oncogenic program, tumor-initiating Club cells reproducibly went through increasing stages of lineage marker conversion across individual tumors within a single mouse and between different mice. A striking characteristic of Club cell-initiated tumor development was the progressive loss of the bronchiolar CC10 marker and the increased gain of the alveolar AT2 cell marker SP-C together with the late onset of Sox2 transcription factor expression, which heralds oncogenic reprogramming and therapeutic resistance.[46-48] Our data thus demonstrate that a subset of KP-transformed Club cells can serve as LUAD-initiating cells and that these cells undergo a progressive process of carcinogenic evolution leading to aggressive and heterogeneous tumor formation.

Accumulating evidence demonstrated that upon *Kras* transformation LUAD can arise from murine AT2 cells.[18,20,23-26] However, as experiments with different K and KP models suggested that Club cells can initiate,[20,27,55] or conversely, fail to initiate LUAD,[18,24,26] the question of whether Club cells are indeed cells-of-origin for LUAD remained controversial. Further confounding the interpretation of previous lineage-tracing experiments with adenoviral-Cre particles, Mainardi and colleagues reported that initial inflammatory stress, caused by adenoviral infection, did modulate the susceptibility of lung epithelial cells to oncogenic transformation.[18] Our study conciliates and extends these reports and provides definitive proof for Club cells as progenitors for LUAD.

To be able to visualize transformed Club cells at single-cell resolution and to investigate their tumorigenic potential over time, we established a model where oncogenic *Kras* expression was restricted to CC10-expressing Club cells (low-dose TAM-induced CKP GEMMs). Importantly, excluding the possibility of inadvertent $Kras^{12V}$ expression in CC10/SP-C dual positive BASCs, the cells that were initially rearranged did not express SP-C protein. Low-dose TAM transgene induction thus specifically targeted Club cells in CKP lungs and circumvented local inflammatory stress, caused by infection with viral particles.

Generalized expression of oncogenic *Kras* in the lungs specifically transformed certain cell types and lineages indicating that only a small fraction of all lung cells can act as progenitors for lung cancer.[14,16,18,20] In CKP lungs, proximal Club cells lining the large airways were completely refractory to $Kras^{12V}$ transformation indicated by the lack of proliferating cells and preneoplastic clusters both at day 12 and at 2 months after transgene activation. Although some $Kras^{12V}$-expressing Club cells at the BADJs did proliferate, the development of preneoplastic areas was completely restricted to the distal bronchioles. These results reveal that Club cells respond differently to oncogenic *Kras* activation and that the potential of Club cells to initiate tumor growth is completely restricted to a subpopulation localized to the distal bronchioles. One intriguing additional finding was that the numbers and anatomical location of proliferating cells were very similar in wild-type and short-term TAM-induced lungs. Since generalized expression of oncogenic Kras in murine lungs promotes tumor formation only in a small subset of cells, it is tempting to speculate that resting lung epithelial cells are not susceptible to transformation and that preceding proliferation is required for productive tumor initiation. However, to prove these two hypotheses, further research will be needed.

Data from different laboratories suggested that oncogenic Kras expression in Club cells could initiate hyperplastic growth patterns but that the tumorigenic potential of these lesions is limited and never progresses beyond the preneoplastic stage.[18,24,26] In contrast to these reports, we demonstrate that Club cell-initiated lesions traverse from preneoplastic AHs, AAHs to ADs and high-grade ACs. Recording

neoplastic hallmarks during tumor development at 2, 4 and 5 months post induction revealed a gradual increase in malignancy over time that finally resulted in an aggressive LUAD phenotype. Because of the very limited immune cell infiltration and the only sporadic but regular appearance of immune cell clusters at the border of late stage tumors, the immune phenotype of Club cell-derived LUAD is best classified as immune-excluded within the time of analysis.[56] Our data thus establish that KP-transformed Club cells undergo a progressive evolution towards aggressive LUAD and that the progressing lesions display an immune cell-excluded phenotype.

In our study, we also define the stepwise histotype conversion of KP-transformed murine Club cells. Immunostaining for the principal bronchiolar and alveolar lineage-defining markers CC10 and SP-C uncovered the progressive loss of the initial CC10 marker and the early onset and increasing gain of the alveolar SP-C marker. Interestingly, analysis of KP-mutated LUAD patients revealed high to intermediate co-expression of CC10 and SP-C in the majority of early stage patients and a decrease of CC10 expression in Stage IV samples. However, taking into account, the small sample size and the fact that the cell-of-origin in these patients remains elusive, this correlative finding should be interpreted with caution. In CKP mice, we also identified some larger tumors with Sox2 protein expression at 4 months after TAM induction and at 5 months, almost all bigger tumors contained Sox2 positive cells. This highly reproducible switch in both lineage-defining markers and the late onset of *Sox2* master transcription factor expression across individual tumors is consistent with the view that initially KP-transformed Club cells undergo a stereotypic carcinogenic program characterized by lineage marker conversion and the late onset of *Sox2* transcription factor expression, involved in oncogenic lineage specification, reprogramming and therapeutic resistance.[46-48] Thus, in line with the long-known cellular diversification of human LUAD[51,52] and the recently reported heterogeneous tumor cell states adopted by progressing KP-transformed AT2 cells,[34,35] our data reveal an inherent plasticity of LUAD-initiating Club cells. The progressing autonomous diversification of Club cell- and AT2 cell-initiated murine lung tumors may also provide a good explanation why individual LUAD cells can survive an initial anticancer treatment and thus facilitate the development of new therapy-resistant phenotypes in human patients.[57] The fact that CC10 single positive LUAD-initiating Club cells localize to the distal bronchioles and almost immediately start to express SP-C also puts in perspective the ongoing debate if BASCs can act as LUAD progenitors in mice. We therefore would like to propose that only a small number of highly plastic epithelial cells, representing a dynamic lineage continuum, is amenable to KP transformation and that this plastic cellular subset resides at the transition of the terminal bronchiole to the alveoli. This view is further supported by recent RNA-sequencing data showing that the murine BASC transcriptome is characterized by promiscuous co-expression of bronchiolar and alveolar epithelial genes and by lineage tracing, demonstrating the potential of BASCs to replenish pools of Club, ciliated, AT1 and AT2 cells upon lung injury.[58,59] The progressive lineage conversion and the late gain of *Sox2* gene expression in Club cell-initiated LUAD also shows that these markers do not reflect the cell-of-origin of murine and possibly also of human LUAD.

In conclusion, our data provide direct experimental evidence for Club cells as cells-of-origin for LUAD. Recording the anatomical localization of LUAD-initiating cells further revealed that only Club cells at the distal bronchioles of the lungs are amenable to KP-transformation and that the trajectory of tumor-initiating cells reproducibly follows a program that is characterized by lineage infidelity, progressive tumor heterogeneity and the final emergence of aggressive LUAD. Given that a subset of murine Club cells can act as progenitors for aggressive KP-initiated LUAD, and supported by recent data demonstrating that genetic ablation of Club cells completely prevented murine lung tumor formation by toxic chemicals found in tobacco smoke,[60] we would like to propose that oncogenic *Kras*-transformed Club cells likely play a major role as LUAD-initiating cells-of-origin in mice and possibly also in humans.

ACKNOWLEDGEMENTS

This work was funded by grants from the Stiftung Rheinland-Pfalz für Innovation (grant number 131838.15) to Ernesto Bockamp and Sebastian Rosigkeit, the PMT-LC—Personalized Multimodal Therapies for the Treatment of Lung Cancer (ERAPERMED2020-342) European network grant to Ernesto Bockamp and Mariano Barbacid, the German Research Foundation (DFG) Collaborative Research Centre (CRC) SFB 1066 (project B3) CRC SFB (project B8) to Detlef Schuppan. We thank Thomas Wacker, Anne Trenkel, Vanessa Schoon and Denise Walscheid for excellent animal care and advice. We also want to acknowledge Prof Dr Susanne Strand, Dr Dennis Strand, Henry Alizor, Henning Janssen and Alexei Nikolaev for their crucial help and advice on generating high-quality microscopic images. Finally, we want to thank Claudia Braun for providing excellent Ki67 immunohistochemistry stains. Our thanks also go to Cristina Sala Ripoll (www.cristinasalaripoll.com) for illustrating Figure 1. Open access funding enabled and organized by Projekt DEAL.

CONFLICT OF INTEREST

The authors declare no conflicts of interest.

DATA AVAILABILITY STATEMENT

The data that support the findings of our study are available from the corresponding author upon reasonable request.

ORCID

Sebastian Rosigkeit https://orcid.org/0000-0003-2431-4066

REFERENCES

1. Siegel RL, Miller KD, Jemal A. Cancer statistics, 2019. *CA Cancer J Clin*. 2019;69:7-34.
2. Travis WD, Brambilla E, Nicholson AG, et al. The 2015 World Health Organization classification of lung tumors: impact of genetic, clinical and radiologic advances since the 2004 classification. *J Thorac Oncol*. 2015;10:1243-1260.
3. Dearden S, Stevens J, Wu YL, Blowers D. Mutation incidence and coincidence in non small-cell lung cancer: meta-analyses by ethnicity and histology (mutMap). *Ann Oncol*. 2013;24:2371-2376.

4. The Cancer Genome Atlas Research Network. Comprehensive molecular profiling of lung adenocarcinoma. *Nature*. 2014;511:543-550.
5. Skoulidis F, Byers LA, Diao L, et al. Co-occurring genomic alterations define major subsets of KRAS-mutant lung adenocarcinoma with distinct biology, immune profiles, and therapeutic vulnerabilities. *Cancer Discov*. 2015;5:860-877.
6. Arbour KC, Jordan E, Kim HR, et al. Effects of co-occurring genomic alterations on outcomes in patients with. *Clin Cancer Res*. 2018; 24:334-340.
7. Aredo JV, Padda SK, Kunder CA, et al. Impact of KRAS mutation subtype and concurrent pathogenic mutations on non-small cell lung cancer outcomes. *Lung Cancer*. 2019;133:144-150.
8. Scheffler M, Ihle MA, Hein R, et al. K-ras mutation subtypes in NSCLC and associated co-occuring mutations in other oncogenic pathways. *J Thorac Oncol*. 2019;14:606-616.
9. Ding L, Getz G, Wheeler D, et al. Somatic mutations affect key pathways in lung adenocarcinoma. *Nature*. 2008;455:1069-1075.
10. La Fleur L, Falk-Sörqvist E, Smeds P, et al. Mutation patterns in a population-based non-small cell lung cancer cohort and prognostic impact of concomitant mutations in KRAS and TP53 or STK11. *Lung Cancer*. 2019;130:50-58.
11. Shepherd FA, Lacas B, Le Teuff G, et al. Pooled analysis of the prognostic and predictive effects of TP53 Comutation status combined with KRAS or EGFR mutation in early-stage resected non-small-cell lung cancer in four trials of adjuvant chemotherapy. *J Clin Oncol*. 2017;35:2018-2027.
12. Kandoth C, McLellan MD, Vandin F, et al. Mutational landscape and significance across 12 major cancer types. *Nature*. 2013;502:333-339.
13. Ruiz-Cordero R, Ma J, Khanna A, et al. Simplified molecular classification of lung adenocarcinomas based on EGFR, KRAS, and TP53 mutations. *BMC Cancer*. 2020;20:83.
14. Guerra C, Mijimolle N, Dhawahir A, et al. Tumor induction by an endogenous K-ras oncogene is highly dependent on cellular context. *Cancer Cell*. 2003;4:111-120.
15. Jackson EL, Olive KP, Tuveson DA, et al. The differential effects of mutant p53 alleles on advanced murine lung cancer. *Cancer Res*. 2005;65:10280-10288.
16. Johnson L, Mercer K, Greenbaum D, et al. Somatic activation of the K-ras oncogene causes early onset lung cancer in mice. *Nature*. 2001; 410:1111-1116.
17. Kim CF, Jackson EL, Woolfenden AE, et al. Identification of bronchioalveolar stem cells in normal lung and lung cancer. *Cell*. 2005; 121:823-835.
18. Mainardi S, Mijimolle N, Francoz S, Vicente-Dueñas C, Sánchez-García I, Barbacid M. Identification of cancer initiating cells in K-Ras driven lung adenocarcinoma. *Proc Natl Acad Sci USA*. 2014;111: 255-260.
19. McFadden DG, Politi K, Bhutkar A, et al. Mutational landscape of EGFR-, MYC-, and Kras-driven genetically engineered mouse models of lung adenocarcinoma. *Proc Natl Acad Sci USA*. 2016;113:E6409-E6417.
20. Sutherland KD, Song JY, Kwon MC, Proost N, Zevenhoven J, Berns A. Multiple cells-of-origin of mutant K-Ras-induced mouse lung adenocarcinoma. *Proc Natl Acad Sci USA*. 2014;111:4952-4957.
21. Westcott PM, Halliwill KD, To MD, et al. The mutational landscapes of genetic and chemical models of Kras-driven lung cancer. *Nature*. 2015;517:489-492.
22. Ferone G, Lee MC, Sage J, Berns A. Cells of origin of lung cancers: lessons from mouse studies. *Genes Dev*. 2020;34:1017-1032.
23. Lin C, Song H, Huang C, et al. Alveolar type II cells possess the capability of initiating lung tumor development. *PLoS One*. 2012;7: e53817.
24. Xu X, Rock JR, Lu Y, et al. Evidence for type II cells as cells of origin of K-Ras-induced distal lung adenocarcinoma. *Proc Natl Acad Sci USA*. 2012;109:4910-4915.
25. Desai TJ, Brownfield DG, Krasnow MA. Alveolar progenitor and stem cells in lung development, renewal and cancer. *Nature*. 2014; 507:190-194.
26. Meuwissen R, Linn SC, van der Valk M, Mooi WJ, Berns A. Mouse model for lung tumorigenesis through Cre/lox controlled sporadic activation of the K-Ras oncogene. *Oncogene*. 2001;20:6551-6558.
27. Cho HC, Lai CY, Shao LE, Yu J. Identification of tumorigenic cells in Kras(G12D)-induced lung adenocarcinoma. *Cancer Res*. 2011;71: 7250-7258.
28. Sutherland KD, Proost N, Brouns I, Adriaensen D, Song JY, Berns A. Cell of origin of small cell lung cancer: inactivation of Trp53 and Rb1 in distinct cell types of adult mouse lung. *Cancer Cell*. 2011;19: 754-764.
29. Xu X, Huang L, Futtner C, et al. The cell of origin and subtype of K-Ras-induced lung tumors are modified by notch and Sox2. *Genes Dev*. 2014;28:1929-1939.
30. Visvader JE. Cells of origin in cancer. *Nature*. 2011;469:314-322.
31. Hoadley KA, Yau C, Hinoue T, et al. Cell-of-origin patterns dominate the molecular classification of 10,000 tumors from 33 types of cancer. *Cell*. 2018;173:291-304.e6.
32. Nagaraj AS, Lahtela J, Hemmes A, et al. Cell of origin links Histotype Spectrum to immune microenvironment diversity in non-small-cell lung cancer driven by mutant Kras and loss of Lkb1. *Cell Rep*. 2017; 18:673-684.
33. Han X, Li F, Fang Z, et al. Transdifferentiation of lung adenocarcinoma in mice with Lkb1 deficiency to squamous cell carcinoma. *Nat Commun*. 2014;5:3261.
34. LaFave LM, Kartha VK, Ma S, et al. Epigenomic state transitions characterize tumor progression in mouse lung adenocarcinoma. *Cancer Cell*. 2020;38:212-28.e13.
35. Marjanovic ND, Hofree M, Chan JE, et al. Emergence of a high-plasticity cell state during lung cancer evolution. *Cancer Cell*. 2020;38: 229-46.e13.
36. Tabbò F, Nottegar A, Guerrera F, et al. Cell of origin markers identify different prognostic subgroups of lung adenocarcinoma. *Hum Pathol*. 2018;75:167-178.
37. Rawlins EL, Okubo T, Xue Y, et al. The role of Scgb1a1+ Clara cells in the long-term maintenance and repair of lung airway, but not alveolar, epithelium. *Cell Stem Cell*. 2009;4:525-534.
38. Marino S, Vooijs M, van der Gulden H, Jonkers J, Berns A. Induction of medulloblastomas in p53-null mutant mice by somatic inactivation of Rb in the external granular layer cells of the cerebellum. *Genes Dev*. 2000;14:994-1004.
39. Rosigkeit S, Meng M, Grunwitz C, et al. Monitoring translation activity of mRNA-loaded nanoparticles in mice. *Mol Pharm*. 2018;15:3909-3919.
40. Robinson SP, Langan-Fahey SM, Johnson DA, Jordan VC. Metabolites, pharmacodynamics, and pharmacokinetics of tamoxifen in rats and mice compared to the breast cancer patient. *Drug Metab Dispos*. 1991;19:36-43.
41. Travis WD, Brambilla E, Noguchi M, et al. International Association for the Study of Lung Cancer/American Thoracic Society/European Respiratory Society international multidisciplinary classification of lung adenocarcinoma. *J Thorac Oncol*. 2011;6:244-285.
42. Yatabe Y, Dacic S, Borczuk AC, et al. Best practices recommendations for diagnostic immunohistochemistry in lung cancer. *J Thorac Oncol*. 2019;14:377-407.
43. Yatabe Y, Mitsudomi T, Takahashi T. TTF-1 expression in pulmonary adenocarcinomas. *Am J Surg Pathol*. 2002;26:767-773.
44. Ikeda S, Naruse K, Nagata C, et al. Immunostaining for thyroid transcription factor 1, Napsin a, p40, and cytokeratin 5 aids in differential diagnosis of non-small cell lung carcinoma. *Oncol Lett*. 2015;9:2099-2104.
45. Chen PM, Wu TC, Cheng YW, Chen CY, Lee H. NKX2-1-mediated p53 expression modulates lung adenocarcinoma progression via modulating IKKβ/NF-κB activation. *Oncotarget*. 2015;6:14274-14289.

46. Bass AJ, Watanabe H, Mermel CH, et al. SOX2 is an amplified lineage-survival oncogene in lung and esophageal squamous cell carcinomas. *Nat Genet*. 2009;41:1238-1242.
47. Tanaka H, Yanagisawa K, Shinjo K, et al. Lineage-specific dependency of lung adenocarcinomas on the lung development regulator TTF-1. *Cancer Res*. 2007;67:6007-6011.
48. Quintanal-Villalonga Á, Chan JM, Yu HA, et al. Lineage plasticity in cancer: a shared pathway of therapeutic resistance. *Nat Rev Clin Oncol*. 2020;17:360-371.
49. Li X, Wang J, Xu Z, et al. Expression of Sox2 and Oct4 and their clinical significance in human non-small-cell lung cancer. *Int J Mol Sci*. 2012;13:7663-7675.
50. Upadhyay VA, Shah KA, Makwana DP, Raval AP, Shah FD, Rawal RM. Putative stemness markers octamer-binding transcription factor 4, sex-determining region Y-box 2, and NANOG in non-small cell lung carcinoma: a clinicopathological association. *J Cancer Res Ther*. 2020; 16:804-810.
51. Oser MG, Niederst MJ, Sequist LV, Engelman JA. Transformation from non-small-cell lung cancer to small-cell lung cancer: molecular drivers and cells of origin. *Lancet Oncol*. 2015;16:e165-e172.
52. Clamon G, Zeitler W, An J, Hejleh TA. Transformational changes between non-small cell and small cell lung cancer-biological and clinical relevance-a review. *Am J Clin Oncol*. 2020;43:670-675.
53. Weinstein JN, Collisson EA, Mills GB, et al. The cancer genome atlas pan-cancer analysis project. *Nat Genet*. 2013;45:1113-1120.
54. Jiang R, Zhang B, Teng X, et al. Validating a targeted next-generation sequencing assay and profiling somatic variants in Chinese non-small cell lung cancer patients. *Sci Rep*. 2020;10:2070.
55. Jackson EL, Willis N, Mercer K, et al. Analysis of lung tumor initiation and progression using conditional expression of oncogenic K-ras. *Genes Dev*. 2001;15:3243-3248.
56. Chen DS, Mellman I. Elements of cancer immunity and the cancer-immune set point. *Nature*. 2017;541:321-330.
57. Marusyk A, Janiszewska M, Polyak K. Intratumor heterogeneity: the Rosetta stone of therapy resistance. *Cancer Cell*. 2020;37:471-484.
58. Salwig I, Spitznagel B, Vazquez-Armendariz AI, et al. Bronchioalveolar stem cells are a main source for regeneration of distal lung epithelia in vivo. *EMBO J*. 2019;38:e102099.
59. Liu Q, Liu K, Cui G, et al. Lung regeneration by multipotent stem cells residing at the bronchioalveolar-duct junction. *Nat Genet*. 2019;51: 728-738.
60. Spella M, Lilis I, Pepe MA, et al. Club cells form lung adenocarcinomas and maintain the alveoli of adult mice. *Elife*. 2019;8:e45571.

SUPPORTING INFORMATION

Additional supporting information may be found online in the Supporting Information section at the end of this article.

How to cite this article: Rosigkeit S, Kruchem M, Thies D, et al. Definitive evidence for Club cells as progenitors for mutant *Kras/Trp53*-deficient lung cancer. *Int. J. Cancer*. 2021; 149(9):1670-1682. https://doi.org/10.1002/ijc.33756